



# Injectable multifunctional CMC/HA-DA hydrogel for repairing skin injury

Longlong Cui<sup>a,1</sup>, Jiankang Li<sup>a,1</sup>, Shuaimeng Guan<sup>a</sup>, Kaixiang Zhang<sup>b</sup>, Kun Zhang<sup>a,\*\*</sup>,  
Jingan Li<sup>c,\*</sup>

<sup>a</sup> School of Life Science, Zhengzhou University, Zhengzhou, 450001, PR China

<sup>b</sup> School of Pharmaceutical Sciences, Zhengzhou University, Zhengzhou, 450001, PR China

<sup>c</sup> School of Materials Science and Engineering, Zhengzhou University, Zhengzhou, 450001, PR China



## ARTICLE INFO

### Keywords:

Full-thickness skin defect repair  
Hydrogel  
Adhesive  
Antioxidant  
Hemostatic

## ABSTRACT

Injectable Hydrogels with adhesive, antioxidant and hemostatic properties are highly desired for promoting skin injury repair. In this study, we prepared a multi-functional carboxymethyl chitosan/hyaluronic acid-dopamine (CMC/HA-DA) hydrogel, which can be crosslinked by horseradish peroxidase and hydrogen peroxide. The anti-oxidation, gelation time, degradability, rheology and antihemorrhagic properties of hydrogels can be finely tuned by varying composition ratio. The cytocompatibility test and hemolysis test confirmed that the designed hydrogel holds good biocompatibility. More importantly, the repair effect of the hydrogel on full-thickness skin injury model in mice was studied. The results of wound healing, collagen deposition, immunohistochemistry and immunofluorescence showed that CMC/HA-DA hydrogel could significantly promote angiogenesis and cell proliferation at the injured site. Notably, the inflammatory response can also be regulated to promote the repair of full-thickness skin defect in mice. Results indicate that this injectable CMC/HA-DA hydrogel holds high application prospect for promising wound healing.

## 1. Introduction

As the body's first line of defense against external stimuli, the skin not only protecting the body from foreign germs, but also sensing stimuli and maintaining homeostasis [1,2]. At the same time, skin is vulnerable to acute trauma, high temperature, chemicals, and other factors, which can cause serious damage [3]. Once severe skin damage occurs, homeostasis of the body would be affected, and the open wound significantly increases the risk of infection [4]. The repair process of skin injury can be divided into four successive stages, which are called hemostasis, inflammation, proliferation and remodeling [5,6]. Most of the minor types of skin defects can be effectively and quickly cured by the human body, but full-layer skin damage is often difficult to cure, and seriously affect people's life and health [7].

In clinic, many full-thickness skin defect would need skin grafts to reduce scar formation of large area and reduce the risk of secondary infection [8]. To speed up the repair of full-thickness skin damage, skin autograft, allograft skin grafts, heterogeneous skin transplantation and amniotic membrane transplantation methods were usually adopted to

achieve therapeutic effect [9]. However, each of these treatment methods have their own limitations, such as the limited source, allogeneic immune rejection, ethical and moral problems, unsatisfactory therapeutic effects, etc. Therefore, a wound dressing product with excellent performance to meet clinical needs is urgent [10,11].

At present, several biomaterials have been designed for wound healing, such as sponges, foams, nanofibers, hydrogels, etc. [12] Especially, injectable hydrogels have many advantages over wound dressings currently on the market, such as three-dimensional porous extracellular matrix structure, ability to provide a moist healing environment, high water content, adjustable mechanical properties, ability to fill irregularly shaped wounds, and good biocompatibility [13–15]. However, many injectable hydrogels cannot have ideal properties such as hemostasis, anti-inflammatory, stimulus response, conductivity, adhesion, anti-oxidation, self-healing, and wound monitoring feature simultaneously [16]. Therefore, it is imperative to develop multifunctional hydrogels.

Hyaluronic acid (HA), as an important component of the extracellular matrix, is a non-sulphated glycosaminoglycan in the human body [17,

\* Corresponding author. School of Materials Science and Engineering, Zhengzhou University, Zhengzhou, 450001, PR China.

\*\* Corresponding author. School of Life Science, Zhengzhou University, Zhengzhou, 450001, PR China.

E-mail addresses: [zhangkun@zzu.edu.cn](mailto:zhangkun@zzu.edu.cn) (K. Zhang), [lijingan@zzu.edu.cn](mailto:lijingan@zzu.edu.cn) (J. Li).

<sup>1</sup> Joint first authors.

18]. Studies have shown that hyaluronic acid is important in cell signal transduction, cell migration promotion and wound healing process [18–21]. In addition, the good biocompatibility, biodegradability, and high hydrophilicity of hyaluronic acid make it an excellent hydrogel material [22]. However, hydrogels with single HA component showed weak adhesion ability [23]. It is known that mussel adhesive proteins can form strong moisture-resistant adhesive bonds, which solidify quickly on various inorganic/organic wet surfaces via the 3,4-dihydroxy-L-phenylalanine (named dopamine, DA). The *ortho*-dihydroxyphenyl (catechol) functional group is the key aspect of DA and its analog dopamine [24]. Inspired by the adhesion chemistry of mussels, DA with catechol group was introduced to improve the adhesion ability. Baolin Guo and co-workers designed a series of injectable adhesive hydrogels based on polydopamine-coated reduction graphene oxide, hyaluronic acid-graft-dopamine (HA-DA), protocatechualdehyde containing catechol and aldehyde groups to promote wound closure and healing. For example, they designed through dual-dynamic-bond cross-linking among ferric iron, protocatechualdehyde and quaternized chitosan to promote methicillin-resistant *Staphylococcus aureus* - infected wound healing [25]. And they used quaternized chitosan, polydopamine-coated reduction graphene oxide, and poly (N-isopropylacrylamide) to develop multifunctional wound dressings [26]. They also synthesized HA-DA by EDC/NHS, and added polydopamine-coated reduction graphene oxide for hydrogels using the horseradish peroxidase (HRP)/hydrogen peroxide (H<sub>2</sub>O<sub>2</sub>) system [27]. What's more, many other works also have shown that DA grafting onto hyaluronic acid molecules could enhance the adhesion ability of hydrogels [28–30].

Hydrogels prepared by physical methods usually have poor stability and are easy to degrade. The hydrogel prepared by chemical method has good mechanical properties, for example, the hydrogels prepared by dopamine and thiol hyaluronic acid through Michael addition reaction have good tissue adhesion *in vitro*, but the introduction of transition metal ions or exogenous coupling agents usually leads to cytotoxicity [31]. The enzymatic crosslinking method allows the reaction to be carried out under mild conditions. A biomimetic dopamine-modified  $\epsilon$ -poly-L-lysine-polyethylene glycol-based hydrogel is prepared by HRP crosslinking [32]. Dopamine modified carboxymethyl cellulose hydrogels were prepared by enzyme crosslinking in the presence of HRP and H<sub>2</sub>O<sub>2</sub> to improve the wet tissue adhesion strength [33]. And dopamine hydrochloride was grafted onto hyaluronic acid coupling by carbodiimide to prepare hydrogels with HRP and H<sub>2</sub>O<sub>2</sub>. [34] Therefore, the HRP/H<sub>2</sub>O<sub>2</sub> enzyme cross-linking method is used to prepare multifunctional hydrogels.

To further improve the cytocompatibility and hemostatic properties, hydrophilic carboxymethyl chitosan (CMC) was added to prepare the hydrogel. In the past two decades, chitosan derivatives have attracted great interest in the fields of biology, pharmacy and medical research. They were used as biomaterials for tissue engineering, drug delivery and wound healing. Introducing carboxymethyl into chitosan structure can significantly increase the solubility of chitosan at neutral and alkaline pH without affecting its properties [35,36]. CMC is holding lots of amino groups, which can enrich and activate negatively charged red blood cells and platelets to stimulate blood coagulation and promote hemostasis [37]. Moreover, CMC can promote the proliferation of fibroblasts and accelerate wound healing [38]. Importantly, the hydrogel formed by CMC can be degraded with the formation of new tissue, and its degradation products hardly cause inflammatory reaction and toxicity [36].

In this paper, HA, DA and CMC were used to synthesize CMC/HA-DA hydrogel by the enzyme cross-linking method with HRP/H<sub>2</sub>O<sub>2</sub>. The greatest advantage that the current approach presents over other reported methods is that we try to obtain a multifunctional hydrogel under mild conditions, which not only has enhanced adhesive, antioxidant and hemostatic ability, but also was injectable, biodegradable and biocompatible, whereas the other reported methods have only showed improvements on some functions or mild conditions. More importantly, in the treatment of full-thickness skin defect model, the hydrogels promoted

rapid wound closure (Fig. 1). This particular combination could be extremely advantageous regarding skin repairing applications.

## 2. Results and discussion

### 2.1. Preparation and characterization of CMC/HA-DA hydrogels

To prepare a cross-linkable hydrogel for improving adhesive property, HA-DA polymer was synthesized with EDC/NHS as coupling agent by the condensation reaction of hyaluronic acid and dopamine in an anaerobic environment at 37 °C. The reaction principle is shown in Fig. 2a. Compared with the hydrogen spectra of HA, a new chemical shift appears in the hydrogen spectra of HA-DA at 6.7 ppm, which is the proton peak of the benzene ring in the catechol group in dopamine (Fig. 2b). The chemical deviation at 2.76 ppm is due to the presence of catechol groups in the benzene-ring methylene group. The water solutions of HA, DA and HA-DA were scanned by UV spectrophotometer in the range of 230 nm–350 nm (Fig. 2c), both DA and HA-DA have stronger UV absorption peaks at 278 nm compared with HA. DA contains catechol groups, which can generate UV absorption at 278 nm, and HA-DA has no other peaks when the wavelength is greater than 300 nm. It shows that there is no oxidation of dopamine. It can be seen that there are –OH stretching vibration absorption peaks in the spectra of HA, DA and HA-DA around 3400 cm<sup>-1</sup> (Fig. 2d). HA contains carboxyl group. The stretching vibration of C–H bond and the asymmetric stretching vibration formed characteristic peaks at 1043 cm<sup>-1</sup> and 1615 cm<sup>-1</sup>, respectively. The asymmetrical stretching vibration peak at 1615 cm<sup>-1</sup> was weakened in HA-DA, and the peak at 1638 cm<sup>-1</sup> indicated that an amide bond was formed between HA and dopamine. All three characterization methods showed that DA was successfully grafted on HA.

Using HRP and H<sub>2</sub>O<sub>2</sub> as catalysts, the injectable hydrogel was prepared by mixing HA-DA solution with CMC solution. Catalase and peroxidase are present in almost all aerobic respiration organisms, and these oxidoreductases play a very important protective role in preventing oxidative damage to cellular components caused by H<sub>2</sub>O<sub>2</sub>, which avoid accumulation of reactive oxygen species (ROS) in cells and regulate their concentration in cellular signaling pathways. HRP is a heme protein, which belongs to a kind of peroxidase and is widely used in the fields of immunochemistry, bio-catalysis, bioremediation and medicine [39]. Horseradish peroxidase is a protein enzyme that can be decomposed by protease, it is usually added in a small amount as an exogenous enzyme, so it has almost no side effects in the body. What's more, the quantitative experiment of residual H<sub>2</sub>O<sub>2</sub> has been done. The experimental results showed that the total amount of hydrogen peroxide used in the preparation of the hydrogel was 2.02 μmol/mL. After the reaction was completed, the hydrogen peroxide content of the hydrogel extract was not within the detection range of the kit. The detection limit of the kit was 0.0027 μmol/mL. Therefore, the residual H<sub>2</sub>O<sub>2</sub> is basically negligible, and there is no need to worry about its possible side effects on the tissue.

In order to characterize the injectable property of CMC/HA-DA hydrogel, the shear thinning parameters of the hydrogel were tested (Fig. 2e). When the shear rate increased linearly from 0.1 to 100 s<sup>-1</sup>, the viscosity of the hydrogel decreased gradually, indicating that the viscosity of the hydrogel decreased with the increase of the shear rate, and the hydrogel had good injectable property [40]. In addition, the hydrogel can be smoothly extruded from the syringe without blockage (Fig. 2f), which also proves that CMC/HA-DA hydrogel is injectable, which enables the hydrogel to closely match the edges of skin lesions and reduce the invasiveness to the surrounding tissues [41]. Fig. 2g showed that CMC/HA-DA hydrogels had a porous three-dimensional network structure which could effectively absorb water and the wound extract. This porous structure also provides channels for the exchange of oxygen, carbon dioxide and nutrients, and provides a good microenvironment for the migration and growth of cells and the remodeling of tissues [42,43].

The gelation mechanism is shown in Fig. 2h. The polymer containing

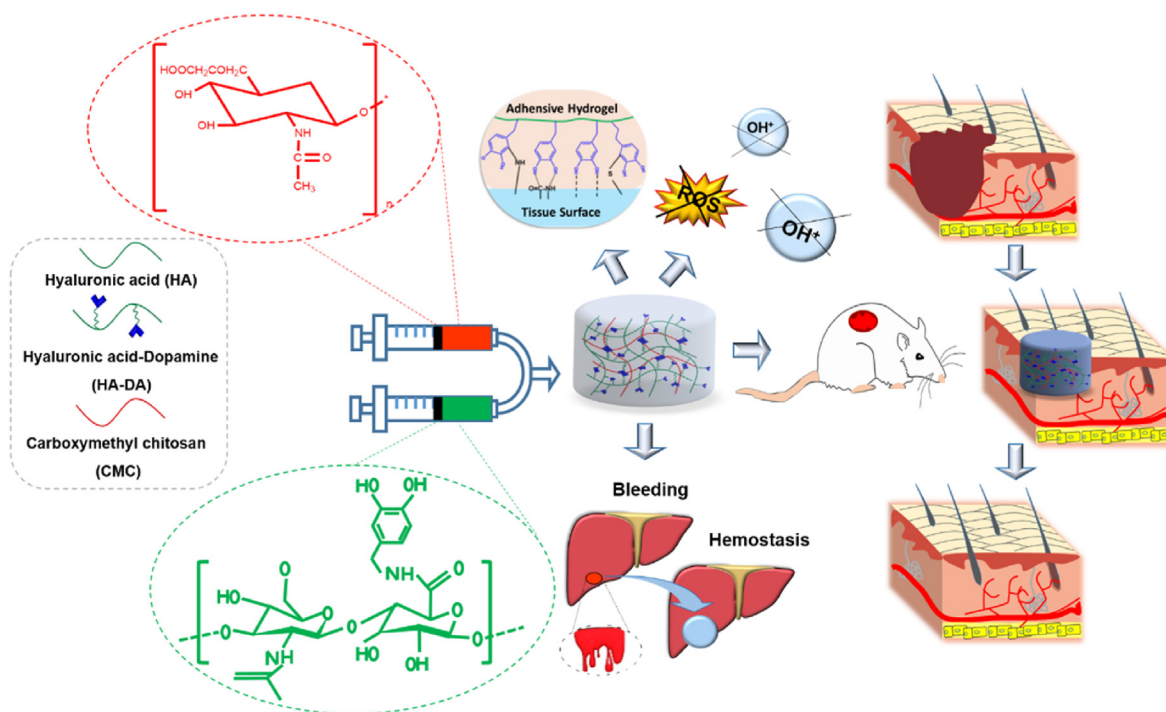


Fig. 1. Schematic illustration of CMC/HA-DA hydrogel for wound repairing.

phenol structure is used as the hydrogen donor in the catalytic process, and  $H_2O_2$  is used as the hydrogen receptor. After the hydrogen donor is oxidized, the hydroxyl group on the benzene ring produces free radicals, and then the free radicals catalyze the C–C bond or C–O bond to bind individual polymers to form gels. In addition, there is an ionic bond between the negative charge of hyaluronic acid and the positive charge of carboxymethyl chitosan, because the positive and negative charges attract each other [44].

## 2.2. Physical and chemical properties of CMC/HA-DA hydrogels

The gelation time of the three groups of hydrogels was 1–5 min, and it was shortened with the increase of HA-DA content (Figure S1 a). The gelation time of CMC/HA-DA<sub>1</sub>, CMC/HA-DA<sub>2</sub> and CMC/HA-DA<sub>3</sub> hydrogels was maintained at  $4.35 \pm 0.3$  min,  $3.3 \pm 0.2$  min, and  $1.58 \pm 0.1$  min, respectively. This set of data mainly proves the influence of the ratio of raw materials on the reaction time. When using this system, before being injected into the body, the reaction solution needs to be mixed thoroughly outside the body for a period of time, and injected into the lesion in situ through a syringe or a pipette. Then the formation of hydrogel can be achieved for in vivo application. Figure. S1 b displayed that the water content of the three groups of hydrogels was all over 95%. High water content indicates high porosity, which is conducive to the transfer of nutrients and metabolites [16].

The network structure of hydrogel is directly related to its mechanical properties. The scanning measurement results of the elastic modulus of CMC/HA-DA hydrogels (Figure. S2). The storage modulus ( $G'$ ) of the three groups of hydrogels was all greater than the loss modulus ( $G''$ ), so the hydrogels had formed a stable structural network within this frequency range. The average storage modulus of the three groups of hydrogels was about 80 Pa, 135 Pa and 230 Pa, respectively. With the increase of HA-DA concentration, the mechanical strength of hydrogel increased, which may be caused by the increase of crosslinking density of hydrogel.

The three groups of hydrogels all appear swelling phenomenon at the initial stage of degradation, indicating that hydrogels have good water absorption and can well absorb the wound extract (Figure.S3 a). All the

three groups of hydrogels could be maintained in the PBS environment for more than 28 days. With the increase of HA-DA concentration, the hydrogels' degradation rate decreased and its stability increased. This indicates that the degradation rate of hydrogels largely depends on the degree of cross-linking.

As shown in Fig.S3 b, the hydrogels of the three groups were completely degraded in 15 U/mL hyaluronidase solution within 24 h, and the degradation rate decreased with the increase of HA-DA concentration. CMC/HA-DA<sub>1</sub> hydrogel, CMC/HA-DA<sub>2</sub> hydrogel, CMC/HA-DA<sub>3</sub> hydrogel was completely degraded at 8 h, 12 h and 24 h, respectively. These results indicate that CMC/HA-DA hydrogel can be degraded by hyaluronidase and has good biodegradability.

Traditional hydrogel dressings are difficult to maintain strong adhesion to the wound site, which easily leads to the shedding of hydrogel dressings. This paper qualitatively tested the adhesion properties and found that the hydrogel could adhere to a variety of inorganic and organic materials (Fig. 3a). According to ASTM F2255-05 (2015), pig skin, as the adhesive substrate material, was used to quantitatively test the shear adhesion strength on the universal material tester (Fig. 3b). The results are shown in Fig. 3c. The shear adhesion strength of CMC/HA-DA hydrogel increases with the increase of HA-DA polymer content. The results showed that the shear adhesion strength of CMC/HA-DA hydrogels with different concentrations was 0.98 kPa, 1.58 kPa and 2.40 kPa, respectively. The change of shear adhesion strength was due to the change of the amount of catechol in dopamine in hydrogels. Medical glue is an emerging medical product to replace needles, it was chosen as control and its main component is cyanoacrylate. The adhesive strength of medical glue reached  $43.47 \pm 4.26$  kPa, much higher than that of hydrogels, mainly because the strength of medical glue after solidification is much higher than that of hydrogel. Compared with the existing literature about hydrogel, the tissue adhesion strength of the hydrogel is lower than other similar hydrogel systems based on dopamine [27], but this does not affect its application. Because wound care varies from different patients. If the wound dressing needs to be changed halfway, the dressing with strong adhesion will cause secondary damage in the removal process. However, if there is no certain adhesion, it will easily fall off during sports, resulting in exposure of wounds and secondary

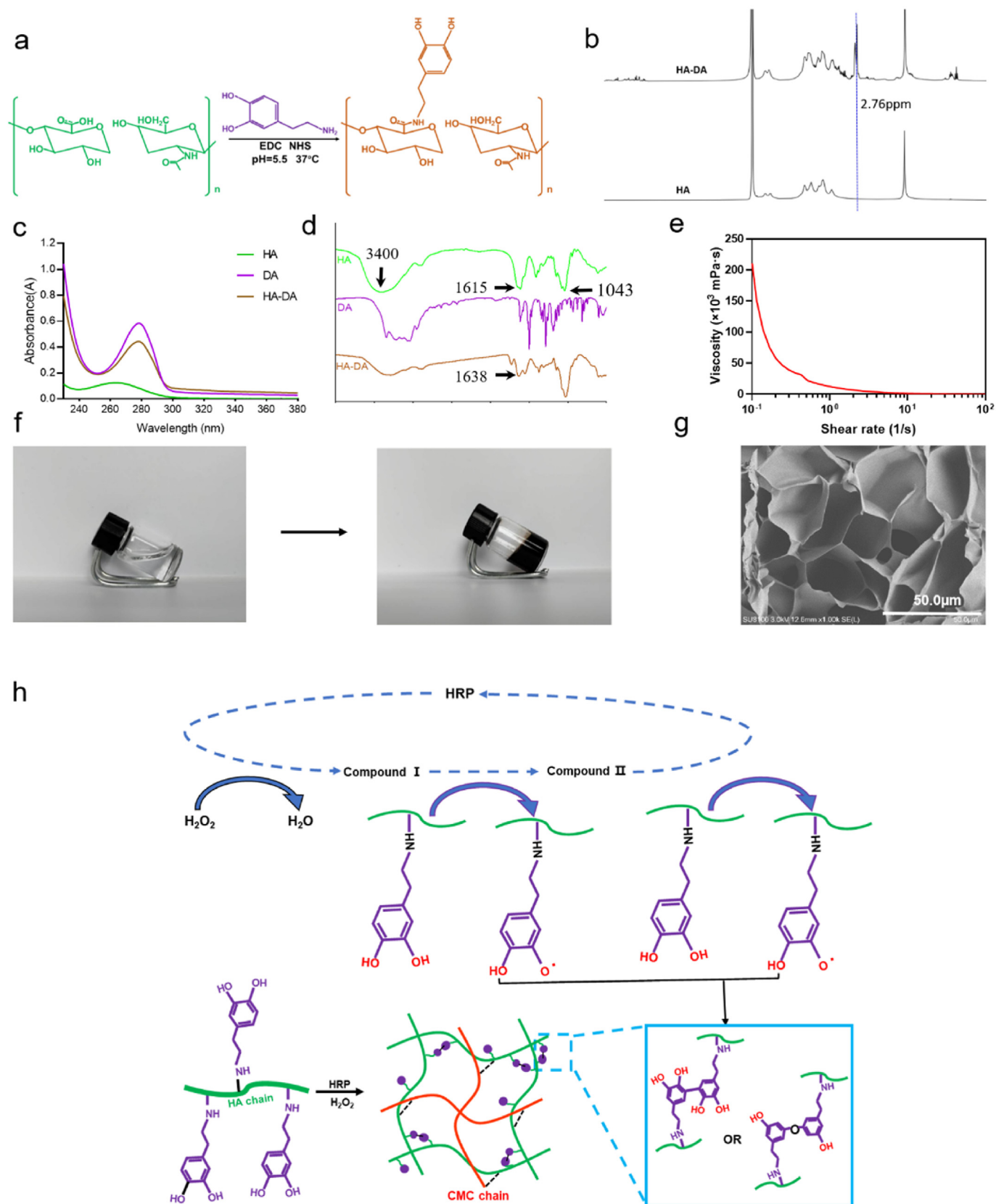


**Fig. 2.** Preparation and characterization of CMC/HA-DA hydrogels. **a.** Composite schematic diagram of HA-DA. **b.**  $^1\text{H}$  NMR data of HA and HA-DA. **c.** Ultraviolet spectra of HA, DA, and HA-DA. **d.** Infrared spectra of HA, DA, and HA-DA. **e.** Rheological behavior of the hydrogel. **f.** Intuitive diagram of the hydrogel formation process. **g.** Internal microstructure of hydrogels. **h.** Schematic diagram of hydrogel gelation principle.

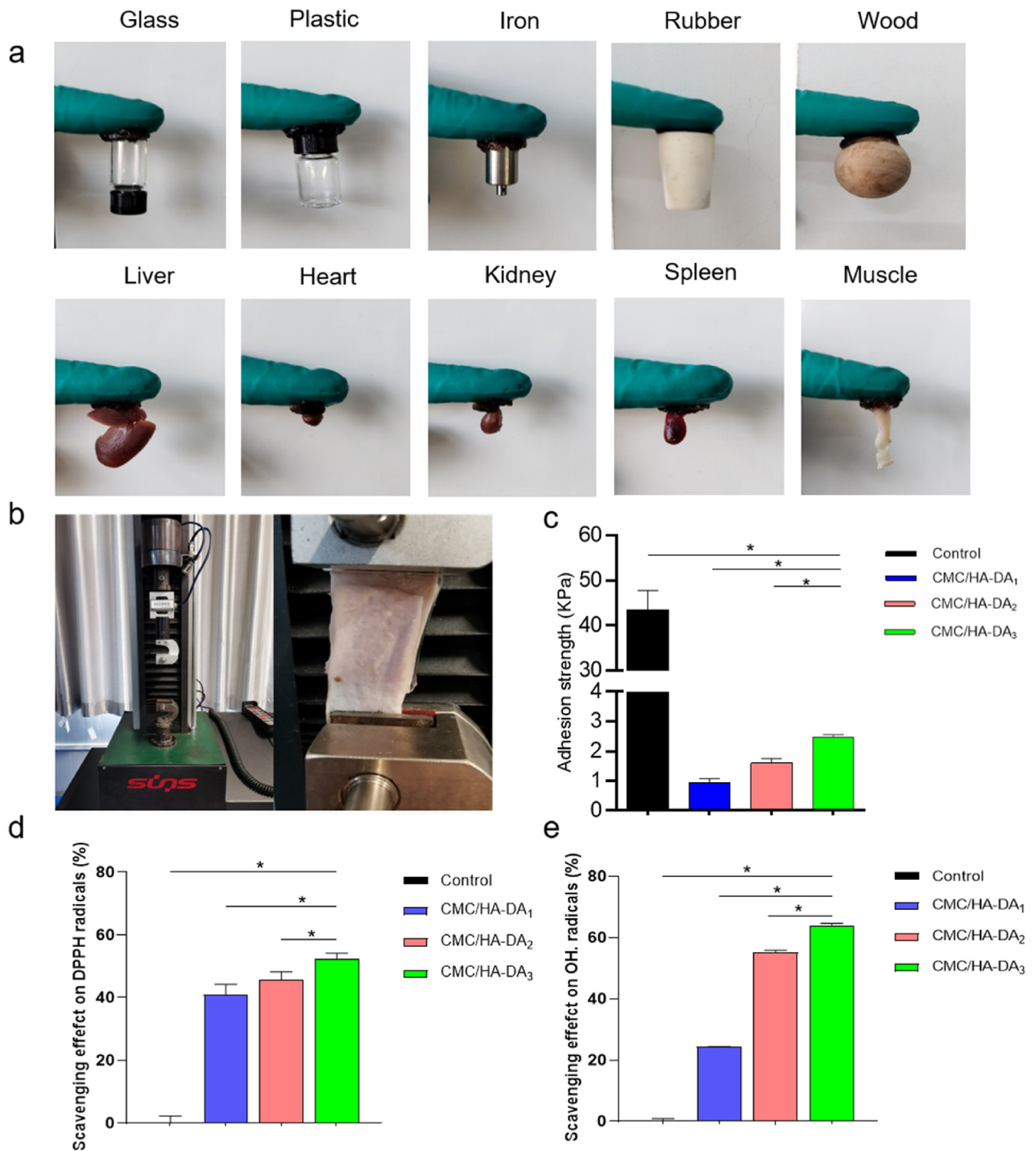


**Fig. 3.** The adhesion and antioxidant property of CMC/HA-DA hydrogels. **a.** Direct view of hydrogel adhesion to various substrate materials. **b.** Hydrogel shear adhesion strength test device diagram. **c.** Figure of the variation of shear adhesion strength of hydrogel with HA-DA concentration (cyanoacrylate as Control). **d.** DPPH free radical scavenging rate of hydrogel (no hydrogel as Control). **e.** The hydroxyl radical scavenging rate of hydrogel (no hydrogel as Control).

injuries. Therefore, multifunctional hydrogels with certain adhesion are clinical needs [45].

In the wound area, inflammation leads to excessive ROS production, which leads to oxidative stress, protein inactivation, cell necrosis, wound infection and a series of phenomena that are not conducive to wound

healing, thus leading to the continuous occurrence of inflammation and the formation of chronic wounds and scars [46–48]. Therefore, antioxidant dressings can promote wound healing by the effective elimination of excessive ROS, which can reduce oxidative stress, improve wound microenvironment, and cell metabolism, and accelerate wound healing

[25]. The antioxidant activity of hydrogels was evaluated by scavenging DPPH and hydroxyl radical. As shown in Fig. 3d and e, all the three groups of hydrogels can scavenge DPPH free radical and hydroxyl free radical, and the scavenging efficiency of the hydrogels is improved with the increase of the content of HA-DA. Among them, the scavenging rates of the hydrogels in the three groups are 41%, 45% and 55% respectively, and the scavenging rates of hydroxyl free radical are 24%, 55% and 65% respectively. CMC/HA-DA hydrogels have excellent antioxidant properties because of a catechol group with antioxidant functions in dopamine [24].

### 2.3. The cytocompatibility of CMC/HA-DA hydrogel

Hydrogel dressings must have good cell compatibility because they are in direct contact with skin wounds and cannot inhibit normal cell proliferation or cause damage to cells [49]. The effect of CMC/HA-DA hydrogel on the proliferation of L929 cells and HaCaT cells was studied. The AM/PI staining method was used to conduct Live/Dead staining to observe the effect of hydrogel on the survival state of the two kinds of cells. The results are shown in Fig. 4a and Fig. 4c. Green fluorescent staining indicates that cells are alive, while red fluorescent staining indicates apoptosis or necrosis. The results showed that on the first and third day, compared with control, there were no large number of apoptotic or necrotic cells in the three hydrogel groups, and the growth morphology of the two kinds of cells did not change. CCK-8 was used to detect the cellular compatibility of the three groups of hydrogels (Fig. 4b and d), the average value of the CCK-8 assay data in the control group was set as 100%, and the ratio of the data in each CMC/HA-DA hydrogel to that in the control group was calculated, then the survival percentage of cells in the hydrogels relative to the control group was obtained. After 24 h and 72 h of co-culture of L929 cells and HaCaT cells with the hydrogels extract of the three groups, the relative survival rates of the two kinds of cells were all greater than 80%. According to the ISO10993-5:2009 biocompatibility test standard, more than 30%

reduction in cell viability is considered a cytotoxic effect [50]. Therefore, the relative cell survival rate of hydrogels proves the good cell compatibility.

### 2.4. The hemocompatibility of CMC/HA-DA hydrogel

In clinical practice, the hemolysis rate of hydrogel materials directly in contact with blood must be within a controllable range, otherwise hemolysis will occur [51]. Then increased levels of free plasma hemoglobin may cause cytotoxic effects, and intravascular hemolysis may induce thrombus or toxicity to other organs. Hemolysis rates of the three hydrogel groups are 0.45%, 0.54% and 0.36% respectively (Fig.S4.). According to the international standard ISO 10993-4, the hemolysis results revealed that the hydrogels did not cause hemolysis [50].

The first stage of wound repair is hemostasis, which is sufficient to illustrate the importance of hemostasis to the overall wound healing process. The coagulability of CMC/HA-DA hydrogel was evaluated by whole blood coagulation experimental model in vitro. A lower BCI indicates a higher degree of clot formation [52,53]. The BCI value of blank group at 4 min and 8 min was  $94\% \pm 3\%$  and  $50\% \pm 2\%$ , respectively, while the BCI value of three hydrogel groups at 4 min was  $51\% \pm 5\%$ ,  $34\% \pm 4\%$ ,  $21\% \pm 6\%$ , respectively (Fig. 5a). CMC/HA-DA<sub>3</sub> hydrogel has the lowest coagulation index, and CMC/HA-DA<sub>3</sub> hydrogel has the lowest coagulation index, and CMC/HA-DA<sub>3</sub> hydrogel has the lowest coagulation index. After 8 min, the coagulation index of the hydrogels in the three groups decreased to  $14\% \pm 2\%$ ,  $8\% \pm 1\%$ ,  $7.5\% \pm 1\%$ , and the coagulation index of CMC/HA-DA<sub>2</sub> hydrogels and CMC/HA-DA<sub>3</sub> hydrogels were both lower than that of CMC/HA-DA<sub>1</sub> hydrogels, and the indexes were similar. Fig. 5b shows the representative images of clots in the pore plates. In the blank group, no obvious clots formed at 4 min, while a small number of clots formed at 8 min. The three hydrogel groups formed obvious clots at 4 min, which became larger with the increase of HA-DA concentration, CMC/HA-DA<sub>3</sub> hydrogel formed the largest clot, but at 8 min, the clot formed by the three hydrogel groups did not have a

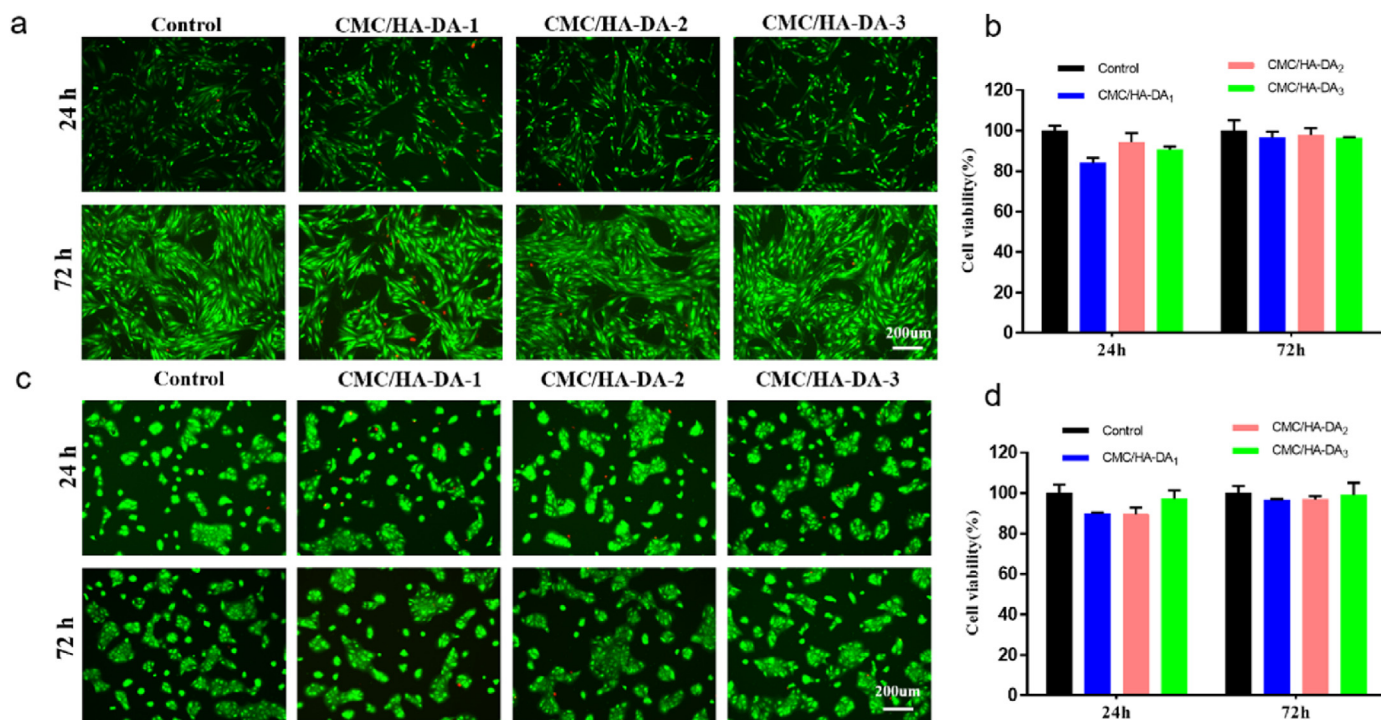
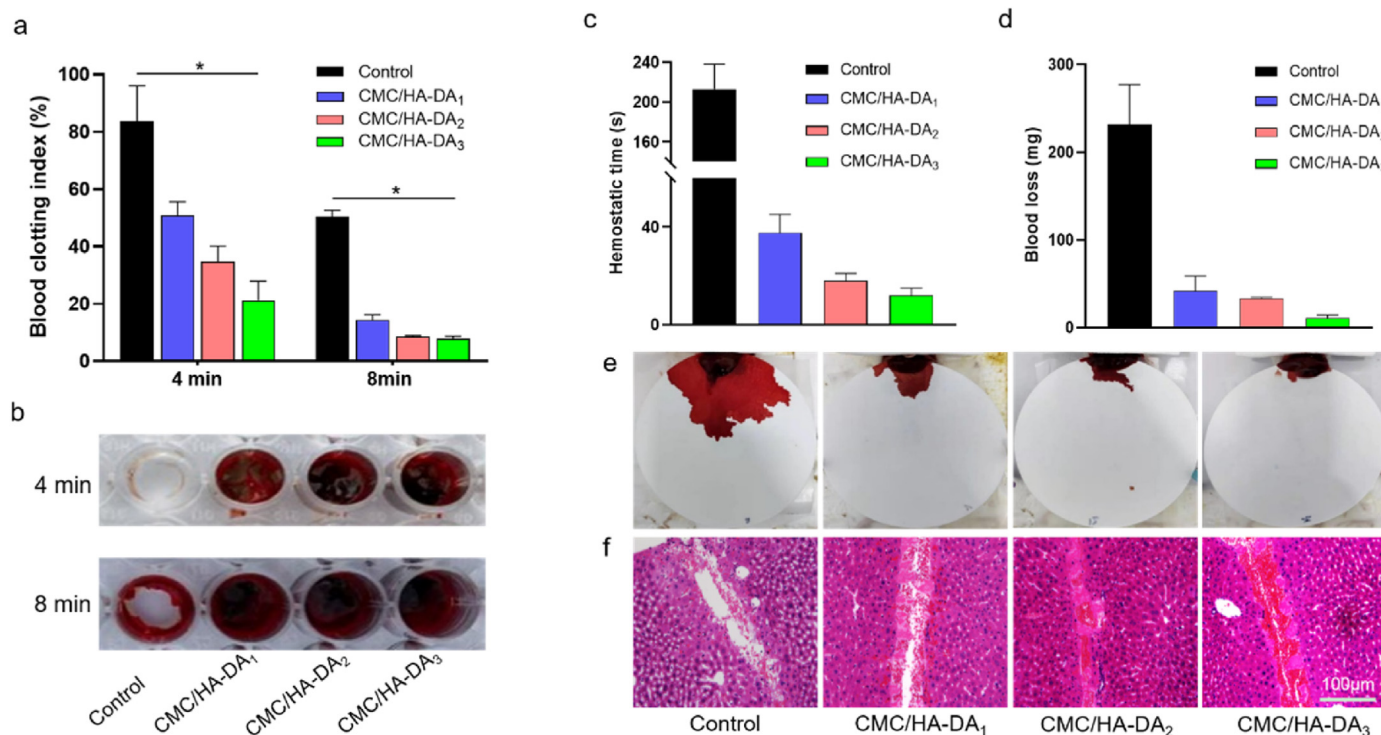


Fig. 4. The good cytocompatibility of CMC/HA-DA hydrogel. a,b: LIVE/DEAD staining and the relative proliferation rate of L929 cells in hydrogel extract for 24 h and 72 h culture. c,d: LIVE/DEAD staining and the relative proliferation rate of HaCaT cells cultured in hydrogel extract for 24 h and 72 h.



**Fig. 5.** The good hemostatic properties of CMC/HA-DA hydrogel. **a.** Blood clotting index of hydrogels at 4 and 8 min, respectively. **b.** Direct view of clot formation. **c.** Statistical chart of hemostasis time. **d.** Statistical chart of final blood loss. **e.** Apparent blood loss of mouse liver. **f.** H&E staining of the liver incision.

significant difference, which was consistent with the experimental results of coagulation index. These results suggest that CMC/HA-DA hydrogels can accelerate clot formation and thus hasten hemostasis and avoid additional blood loss.

The study of grafting dopamine hydrochloride onto hyaluronic acid and preparing hydrogels with horseradish peroxidase and H<sub>2</sub>O<sub>2</sub> as triggers showed the effect of promoting hemostasis [34], in this paper, it can speed up hemostasis and reduce bleeding quantity after adding CMC. The hemostatic performance of hydrogel *in vivo* was evaluated by the experimental model of hepatic hemorrhage in mice (Fig. 5c and d). For the blank group, CMC/HA-DA<sub>1</sub> hydrogel, CMC/HA-DA<sub>2</sub> hydrogel and CMC/HA-DA<sub>3</sub> hydrogel, the hemostasis time of the hydrogels was maintained at 210 ± 30 s, 38 ± 8 s, 18 ± 3 min, and 12 ± 3 min; the final blood loss was 230 ± 30 mg, 42 ± 10 mg, 33 ± 2 mg and 11 ± 4 mg. It can be seen from the results that hydrogel can significantly shorten the hemostasis time and reduce the amount of blood loss. In addition, the H&E staining results (Fig. 5f) of the liver bleeding site showed that in the hydrogel treatment group, many red blood cells without nuclei gathered at the injury site, and the CMC/HA-DA<sub>3</sub> hydrogel had the largest amount of blood cells, indicating that hydrogel could significantly induced the aggregation of blood cells at the wound site and induce blood coagulation, thus reducing blood loss.

## 2.5. Wound healing assay *in vivo* and histological analysis

Grafting DA onto HA enables HA-DA-based hydrogels with good adhesion, hemostatic ability and antioxidant properties [24,27]. A mouse full-thickness skin defect repair model was used for simulation experiments to confirm the role of CMC/HA-DA hydrogel as wound dressing in animal experiments. Based on the physical and chemical properties, cytocompatibility and hemocompatibility, it was shown that CMC/HA-DA<sub>3</sub> hydrogel was the best one, which means that the properties can be adjusted with the concentration of HA-DA, and the higher of the concentration, the better properties will be observed. But we also considered the gelation time in animal experiments to achieve

operability. Therefore, in the present laboratory situation, CMC/HA-DA<sub>2</sub> hydrogel was selected as the representative sample of animal experiments to prove its versatile and effective. After modeling the wounds on the back of mice, CMC/HA-DA hydrogel was injected into the wounds *in situ*. The Control group was treated with normal saline. The Tegaderm™ film group was covered with the wound dressing sold by Tegaderm™ film. At the 3rd, 7th and 14th day after treatment, the wound healing of the mice was photographed and recorded. The results are shown in Fig. 6. The wound healing photos taken on the third day after treatment showed that the wound healing effect of the hydrogel group was better than that of the control group and the Tegaderm™ film group at the early stage of wound healing. The wound healing rate of hydrogel group was about 55%, while the wound healing rate of Control group and Tegaderm™ film group was only 20% and 32%. On the 7th day, the hydrogel group's wound healing rate reached 77%, while that of the Control group and the Tegaderm™ film group was 42% and 50%. On the 14th day, the wounds on the back of mice in the hydrogel group were almost completely healed, while 28% and 20% of the wound areas in Control group and Tegaderm™ film group were still not healed. The results proved that CMC/HA-DA hydrogel could better promote the repair of full-thickness skin injury in mice.

Granulation tissue formed by fibroblasts, matrix remodeling and growth factors is an important indicator of wound healing. Thicker granulation tissue indicates faster wound healing [26]. On the 7th and 14th day after treatment, new tissue sections were taken from the wound site for staining, respectively. H&E staining was used to evaluate the skin regeneration at the wound site, and Masson's Trichrome staining was used to analyze collagen deposition at the wound regeneration site. The results of H&E staining and the quantitative analysis are shown in Fig. 7a and Fig. 7c. In the hydrogel treatment group, the wound healing was more complete, with obvious re-epithelialization, granulation tissue formation and new skin attachment formation. Collagen deposition can provide mechanical support for new tissues and promote cell proliferation and differentiation, which is important in the process of wound healing. According to Masson's Trichrome staining results (Fig. 7b and d),

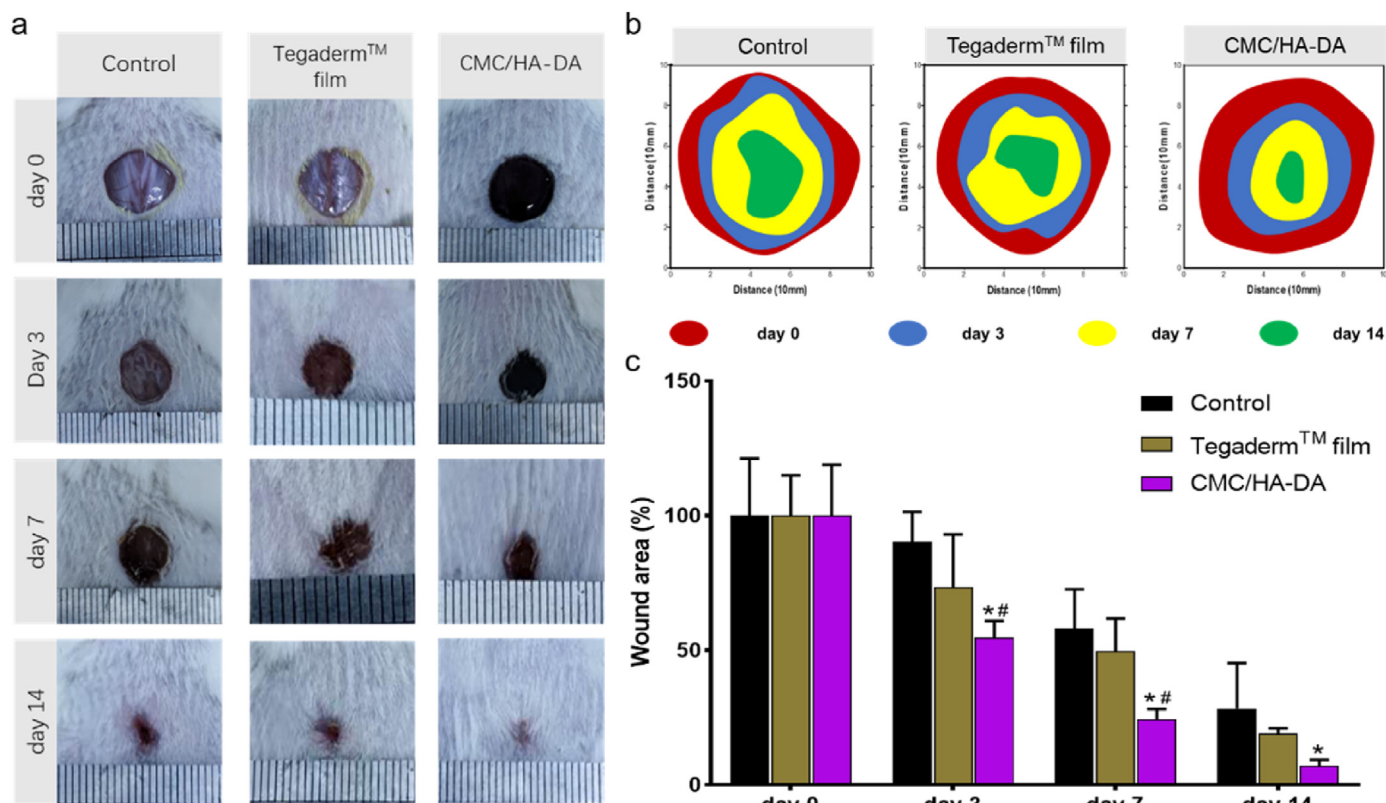


**Fig. 6.** The wound repair promotion ability of CMC/HA-DA hydrogel. **a.** Direct wound healing chart of mice. **b.** Schematic diagram of the wound area of the damaged skin of mice over time. **c.** Wound area residual rate.

the blue color of the wound treated with hydrogel is more intense than Control group and Tegaderm™ film group. It shows that the collagen deposits are thickest, densest, and most evenly arranged. The curative effect of Tegaderm™ film group was not obvious, mainly because when the wound was wet, the film was easily attached to the wound to prevent bacteria. However, when the wound was scabbed, the Tegaderm™ film was easy to fall off, and it was difficult for a new film to be attached. However, due to the good adhesion properties, the hydrogel had been integrated with the wound when the wound was scabbed, and continuously promoted the healing of the wound. Therefore, the curative effect was remarkable.

## 2.6. Expression analysis of neovascularization marker protein and inflammatory factors

Numerous studies have shown that the process of wound healing involves not only hemostasis and matrix remodeling, but also inflammation and angiogenesis [27]. Many marker proteins and cytokines can be used to detect changes in the wound microenvironment.  $\alpha$ -SMA is commonly used as a phenotypic marker for vascular smooth muscle cells and can reflect the newly formed blood vessels in regenerated tissues [54]. The results showed (Fig. 8a) that more  $\alpha$ -SMA positive cells were expressed in the skin wound healing site of the hydrogel group than Control group and Tegaderm™ film group, which indicated that CMC/HA-DA hydrogel could promote angiogenesis in new tissue.

Overexpression of MMP-9 can interfere with the formation of granulation tissue, leading to poor wound healing, and its expression level is significantly increased in chronic inflammation [55,56]. Immunohistochemical staining was used to analyze the inflammation of the wound site, and the results are shown in Fig. 8b. The positive expression of MMP-9 in the hydrogel group was less, indicating that the wound site inflammation was less than Control group and the Tegaderm™ film group.

CD31 is a biomarker of vascular endothelial cells and angiogenesis [57]. immunofluorescence staining results showed (Fig. 8c) that the hydrogel group of CD31 positive expression of injury is more intense, new blood vessels were more and their injury density was higher, with tube cavity structure. According to the CD31 staining results in the wound site, the number of new blood vessels per square millimeter area was significantly different. Statistical number of new blood vessels in the hydrogel group was higher than the Control group and the Tegaderm™ film group. These results were consistent with the above immunohistochemical  $\alpha$ -SMA staining results, which proved that hydrogel could significantly promote vascular regeneration in the injured site. To better understand the effect of hydrogel on wound repair, we evaluated cell proliferation at the wound site by detecting the expression level of PCNA. On the 14th day, PCNA protein in the hydrogel group was significantly expressed higher than that in Control group and Tegaderm™ membrane group, indicating that hydrogel can promote cells proliferation in the injured site, thus promoting wound healing.

The expressions of inflammation-related proteins IL-6, IL-10 and angiogenic marker VEGF at the skin injury sites of mice were detected by Western blotting after 14 days of postoperative treatment (Fig. 9). VEGF in the hydrogel group was significantly expressed higher than that in Control group and Tegaderm™ film group ( $P < 0.05$ ). This indicated that hydrogel effectively promoted the angiogenesis of the injured site, which was consistent with the above results of  $\alpha$ -SMA immunohistochemical detection and CD31 immunofluorescence detection. Among the three groups, the expression of pro-inflammatory cytokine IL-6 was significantly down-regulated in the hydrogel group, while the expression of anti-inflammatory cytokine IL-10 was significantly up-regulated, with statistical significance ( $P < 0.05$ ), indicating that CMC/HA-DA hydrogel can reduce the inflammatory response and is beneficial to wound repair. Collectively, these results showed that CMC/HA-DA hydrogel has properties of inhibiting inflammation and promoting angiogenesis.

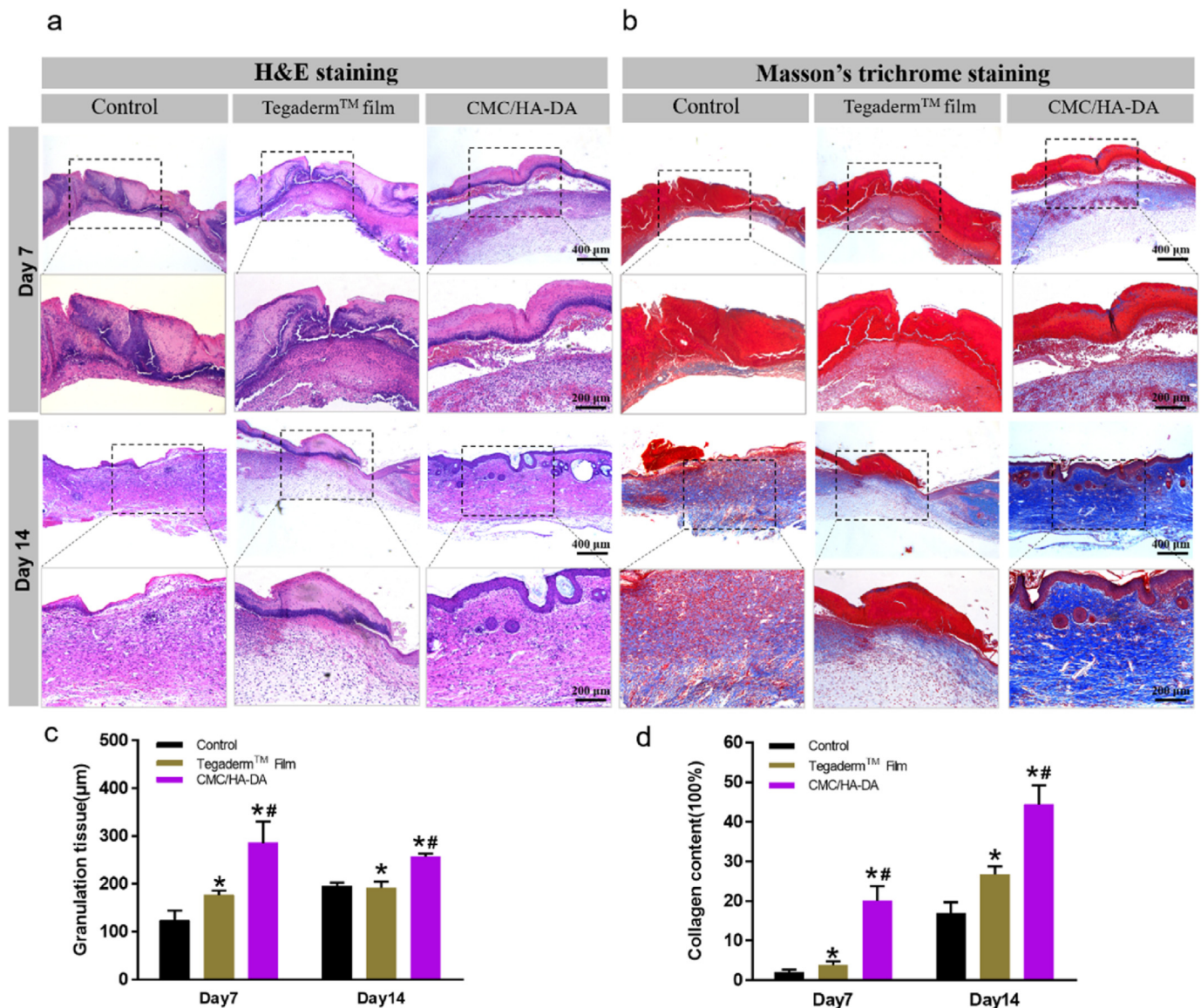


Fig. 7. Remodeling tissue staining of CMC/HA-DA hydrogel group. The histopathological changes of skin wounds (a) and its quantitative analysis (c) on the 7th and 14th day. Masson's Trichrome staining of skin wounds (b) and its quantitative analysis (d) on the 7th and 14th day.

### 3. Materials and methods

#### 3.1. Materials

Carboxymethyl chitosan and horseradish peroxidase were purchased from Solarbio (Beijing, China). All the antibodies were bought from Proteintech Group Inc (Wuhan, China). Dopamine hydrochloride, Hyaluronic acid (MW =  $5 \times 10^5$  Da), Calcein-AM, 1-ethyl-3-(3-dimethylaminopropyl)-carbodiimide (EDC) and N-hydroxy succinimide (NHS) were purchased from Sigma Aldrich (St Louis, USA).

#### 3.2. Synthesis of HA-DA polymer

HA solution was prepared with HA (1 g) and 100 mL of deionized water. The HA solution was activated with EDC (1162 mg) and NHS (862 mg) for 30 min, and then dopamine hydrochloride (1425 mg) was added to the reaction system. The pH of the reaction system was adjusted to 5.5 by HCl and NaOH, and the reaction was carried out under nitrogen protection at 37 °C for 24 h. After the reaction, HA-DA was obtained by

using a dialysis membrane (MWCO ~ 8000 Da) for 72 h and then freeze-drying.

1% HA-DA was characterized by  $^1\text{H}$  NMR spectroscopy (600 MHz NMR spectrometer, AVIII HD 600, Switzerland), fourier transform infrared spectroscopy (FTIR, TENSOR 27, BRUKER, Germany), and UV absorption profiles at 230–350 nm (UV-vis-NIR spectrophotometer, UV-3600 plus, Japan).

#### 3.3. Preparation and characterization of CMC/HA-DA hydrogels

The HA-DA solution with the concentration of 2%, 4% and 6% and the CMC solution (6%) with the volume ratio of 1:1 was fully mixed, HRP and  $\text{H}_2\text{O}_2$  were used as catalysts to prepare hydrogels with three different raw material ratios [58]. The hydrogels were named as CMC/HA-DA<sub>1</sub>, CMC/HA-DA<sub>2</sub>, CMC/HA-DA<sub>3</sub>.

The internal morphology of CMC/HA-DA hydrogels after freeze-drying, fracture and gold-spraying was characterized by scanning electron microscopy (SEM, FEI Quanta200, The Netherlands).

The gelation time was measured by tilt method. At 37 °C, HA-DA and

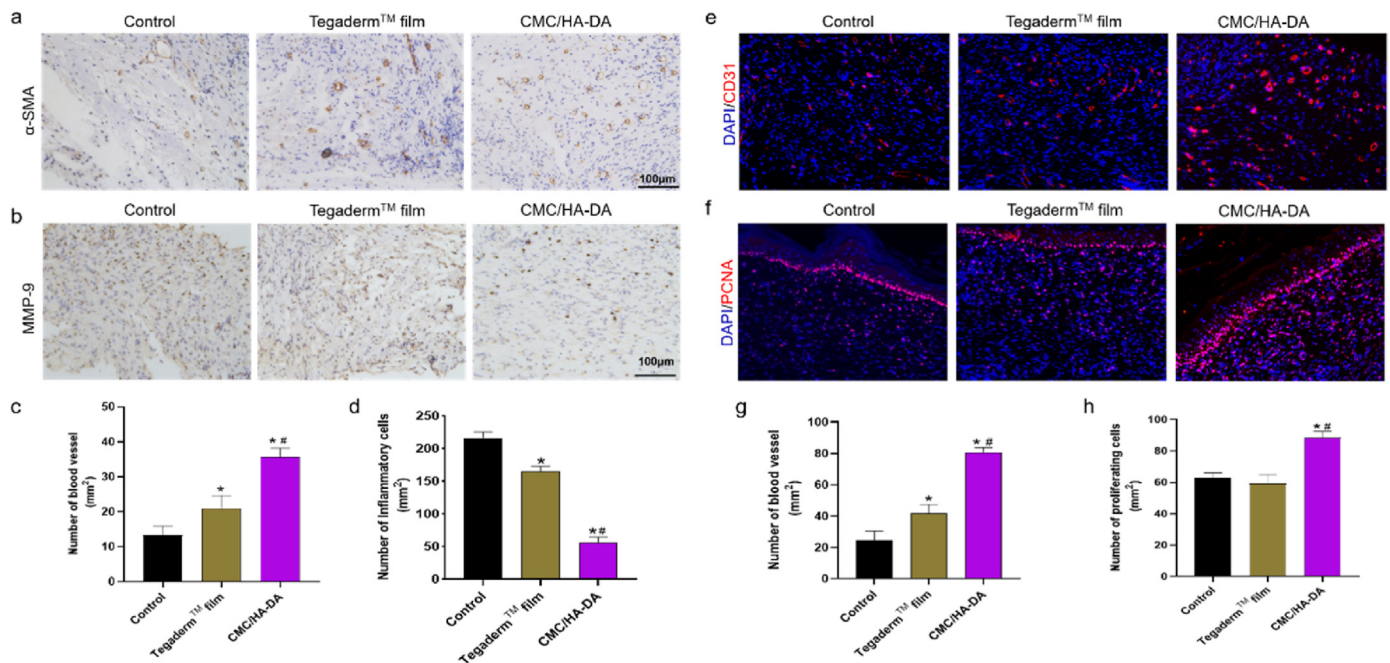


**Fig. 8.** Immunohistochemical and immunofluorescence analysis of regenerated wound tissue. **a.** The expression of  $\alpha$ -SMA in the skin wound of each group on the 14th day. **b.** The expression of MMP-9 in the skin wound of each group on the 14th day. **c.** Quantified data of the relative area percentage of number of blood vessel. **d.** Quantified data of the relative area percentage of number of Inflammatory cells. **e.** The expression of CD31 in the skin wound of each group on the 14th day. **f.** The expression of PCNA in the skin wound of each group on the 14th day of treatment. **g.** Quantified data of the relative area percentage of number of blood vessel. **h.** Quantified data of the relative area percentage of number of proliferating cells.

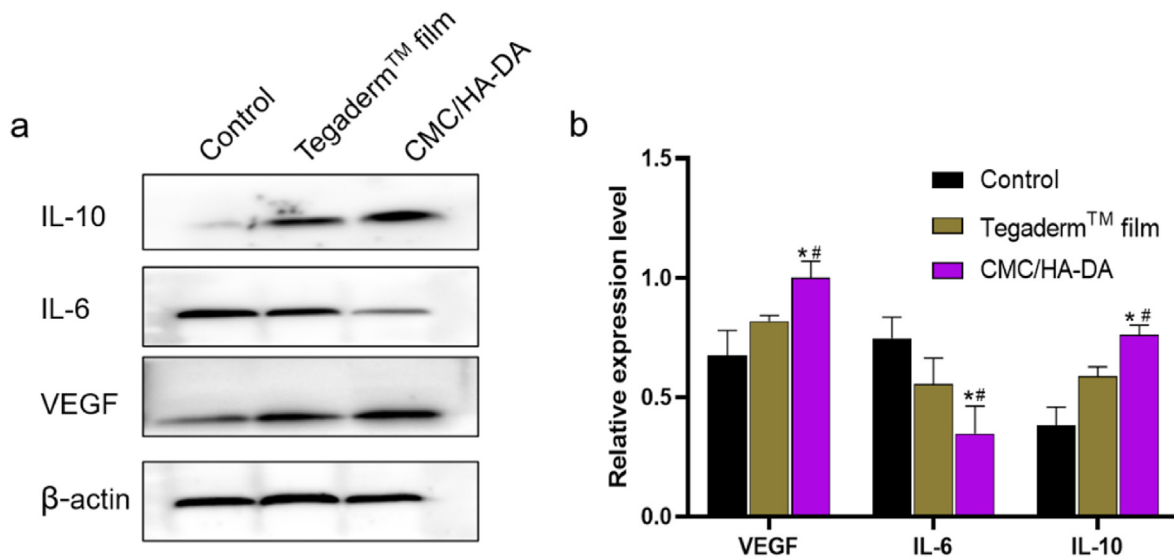


**Fig. 9.** Western blotting of regenerated wound tissue. **a.** The expression of related proteins at the injured site of mice on the 14th day of treatment. **b.** The gray scale analysis and quantification of related proteins.

CMC solutions were mixed and HRP/H<sub>2</sub>O<sub>2</sub> were added. The timing was started and the vial was tilted to observe the mixed solution every 5 s until the liquid stopped flowing, and the gelation time was recorded.

The water content (WC) of hydrogels was also measured by  $WC (\%) = [(W_w - W_d)/W_w] \times 100\%$ , where  $W_w$  and  $W_d$  are the hydrogels' weight after 24 h of swelling and drying, respectively.

### 3.4. Rheological property and stability of hydrogels

Rheological properties of CMC/HA-DA hydrogels were assessed by measuring their elastic modulus via a rheometer platform (TA DHR2,

USA). The specific parameters were set as: dynamic oscillation scanning frequency was 1 Hz–100 Hz, temperature was 37 °C, strain was 1%. The shear viscosity of the CMC/HA-DA hydrogels was determined by increasing the shear rate from 0.01 to 100 s<sup>-1</sup>. The linear viscoelastic range was measured at a fixed frequency of 10 rad/s with a strain sweep (0.01–100%).

The prepared 100  $\mu$ L hydrogel was placed in a PE tube containing 1 mL PBS under 37 °C water bathing. The remaining mass of hydrogel was measured at 1, 3, 5, 7, 14, 21 and 28 days, denoted as  $W_t$  and original mass as  $W_0$ . The degradation rate of hydrogel was calculated according to formula  $L = [(W_0 - W_t)/W_0] \times 100\%$ .

Hydrogels were put in a PE tube including 15 U/mL hyaluronidase, and placed in water bathing at 37 °C. Hydrogels were taken out at 2, 4, 6, 8, 10, 12 and 24 h, and the quality of the hydrogel was recorded as  $W_t$ . Then new hyaluronidase was replaced until the hydrogels were completely degraded. The enzymatic hydrolysis rate of hydrogel was calculated following  $E = [(W_0 - W_t)/W_0] \times 100\%$ .

### 3.5. Adhesion property of hydrogels

Qualitative characterization of the adhesion properties of hydrogels to different materials: inorganic materials (glass, plastic, iron, rubber, wood) and organic materials (heart, liver, spleen, lung, kidney, muscle) were selected as the base materials for visual detection.

Quantitative test on the adhesion ability of hydrogels to host tissues: Fresh pig skin was used as the substrate, and the shear adhesion test of hydrogels was conducted according to ASTM F2255-05 (2015). First, a fresh pig skin is soaked in alcohol to remove the fat layer, then sheared into rectangles of 50 mm × 25 mm and soaked in PBS for use. Two pig skin samples were selected and the hydrogel was injected into the surface of the pig skin samples with an area of 25 mm × 10 mm. Then the two pig skins were bonded together, and the lap shear test was done in the tensile mode on the universal material tester with a rate of 5 mm/min. The maximum tensile force  $N_{max}$  was recorded. The shear adhesion strength of hydrogels can be obtained according to the following formula:

$$P_a = N_{max}/m^2$$

Where,  $P_a$  is the shear viscosity strength, and  $m^2$  is the overlap area of hydrogel on pig skin, i.e., 250 mm<sup>2</sup>.

### 3.6. ROS scavenging activities of hydrogels

The hydroxyl radical scavenging assay was performed by employing the Fenton reaction. Firstly, 300 μL CMC/HA-DA<sub>1</sub>, CMC/HA-DA<sub>2</sub> and CMC/HA-DA<sub>3</sub> hydrogels were prepared respectively, and incubated with a mixture of FeSO<sub>4</sub> solution and saffron O solution for 10 min. After H<sub>2</sub>O<sub>2</sub> solution was added, the mixture was reacted at 55 °C for 60 min. The absorption value  $A_1$  of the mixed solution at 492 nm was measured by ultraviolet spectrophotometer. In blank group, 300 μL ddH<sub>2</sub>O was used and the absorption value was denoted as  $A_0$ ; in control group, 300 μL ddH<sub>2</sub>O and 800 μL H<sub>2</sub>O<sub>2</sub> were used, and the absorption value was denoted as  $A_2$ . The hydroxyl radical scavenging rate of hydrogels was calculated using the following formula:  $ROH = [(A_1 - A_0)/(A_2 - A_0)] \times 100\%$

The DPPH free radical scavenging ability of hydrogel was also determined. The specific procedure was to disperse 100 μmol DPPH and 300 μL hydrogel in 3 mL of anhydrous ethanol. Then stir the mixture well and let it react in the dark for 30 min. Next, the absorption value  $A$  of the mixture at 517 nm was detected by ultraviolet spectrophotometer. The DPPH clearance rate was calculated by the following formula:  $R_{DPPH} = [(A_1 - A_2)/A_1] \times 100\%$

$A_1$  represents the absorption value of blank group (DPPH + anhydrous ethanol), and  $A_2$  represents the absorption value of hydrogel group (DPPH + anhydrous ethanol + hydrogel).

### 3.7. Cytotoxicity of the hydrogels

L929 and HaCaT were selected as experimental cells. Logarithmic growth cells were cultured at  $2.3 \times 10^3$  (L929) and  $2.5 \times 10^3$  (HaCaT) cell densities in 96-well plates for 24 h in a cell incubator. At the same time, the materials needed to synthesize the hydrogel were sterilized in advance for 30 min, and 100 μL hydrogel was prepared on the ultra-clean platform, and then it was put into 1 mL RPMI-1640 cell culture medium for 24 h, the culture medium was sucked out, and the new medium was added to the control group, while the original cell culture medium was replaced by hydrogel extract in the experimental group for 24 h and 72 h.

After cell culture, CCK-8 and Live/Dead staining were used to detect the cell proliferation in hydrogels.

### 3.8. Hemolytic and hemostatic properties of the hydrogels

The hemolysis rate (HR) of CMC/HA-DA hydrogel was measured by the method in the literature [59]. HR was calculated following the formula:  $HR = [(D_s - D_n)/(D_p - D_n)] \times 100\%$ ,  $D_s$ ,  $D_p$ , and  $D_n$  represent the absorbance of the sample, the distilled water mixed with samples, and normal saline mixed with samples respectively.

The blood coagulation effects of different CMC/HA-DA hydrogels were tested using whole blood in vitro. Fresh whole blood of mice was observed with anticoagulant tubes. The prepared 50 μL hydrogel samples were placed in the 96-well plate, and then the samples were rinsed with normal saline for 3 times. Add 50 μL whole blood to each well, and then 5 μL 0.2 M CaCl<sub>2</sub> to form fibrin clots. After incubation for 4 and 8 min at 37 °C, the fibrin clots were washed with 100 μL saline carefully added along the well wall, washed for 20 times, and then 2 mL supernatant was collected. Hydrogel-free pores served as the control group. The absorbance values of supernatants of the hydrogel group and the control group at 540 nm were measured by enzyme plate analyzer, which were recorded as  $A_V$  and  $A_N$ , respectively. The absorbance value of whole blood diluted with 2 mL normal saline (50 μL) at 540 nm was taken as the reference value, denoted as  $B$ . The blood clotting index (BCI) in vitro was calculated using the formula.  $BCI = A/B \times 100\%$ .

To evaluate the hemostatic ability of CMC/HA-DA hydrogel in vivo, the Kunming mouse model of liver hemorrhage was used for the experiment. In brief, the anesthetized mice using 10% chloral hydrate were fixed on a test bench with an incision exposing the liver. Liver bleeding was induced with a 20 g needle, and the angle between the test table and the horizontal plane was 30°, which was convenient for blood adsorption to the filter paper placed under the liver. Then 100 μL of different CMC/HA-DA hydrogel was quickly applied to the wound and the hemostasis time was recorded, and the filter paper's weight was measured. Tissues around the liver incisions were used for hematoxylin and eosin (H&E) test.

### 3.9. In vivo tests

The animals were approved by the institutional review board of Zheng Zhou University. Female Kunming mice (25–35 g, 5–6 weeks) were used for 3 groups including control, Tegaderm™ film, CMC/HA-DA hydrogel. Each group contained 8 mice. Skin injury modeling was performed on a sterile operating table. Experimental mice were anesthetized by intraperitoneal injection of chloral hydrate. The back area of the mouse was shaved in preparation for subsequent modeling. A full thickness skin wound with a diameter of 8 mm was made on the back of the mouse. After skin removal, hydrogel was added to the wound as the hydrogel group, and Tegaderm™ film (3 M Health Care, USA) was added to the wound, while the control group was not treated. The wound healing data was collected on the 3rd, 7th, and 14th day after surgery.

On the 7th and 14th day of the experiment, the mice in each group were sacrificed to take the specimens from the healed wounds. The tissue samples were fixed, embedded, cross sectioned, and stained with H&E and Masson's trichrome. On the 14th day The primary α-SMA and MMP-9 antibody (Servicebio, China, 1:2000) were used for immunohistochemical staining. CD31 (Servicebio, China, 1:200) and PCNA (Servicebio, China, 1:200) antibodies were used for immunofluorescent staining. The primary antibodies rabbit polyclonal VEGF (Proteintech, China, 1:1000), IL-6 (Proteintech, China, 1:1000), and IL-10 (Proteintech, China, 1:1000) were used for Western blotting.

### 3.10. Statistical analysis

ANOVA was used to analyze the experimental results. Image J was used for grayscale analysis. Error bars presented mean ± standard

deviation (SD), and \* $p < 0.05$  was regarded to be significant difference.

#### 4. Conclusions

In summary, we propose a novel composite hydrogel, which is prepared by the enzyme cross-linking method with HRP/H<sub>2</sub>O<sub>2</sub>, using carboxymethyl chitosan and dopamine grafted hyaluronic acid. CMC/HA-DA hydrogels not only exhibit multifunctional like injectability, porous network structure, adjustable gelling time, high water content, good biodegradability and biocompatibility, but also has good tissue adhesion, excellent antioxidant and hemostatic properties. CMC/HA-DA hydrogel can accelerate wound healing with high collagen deposition, granulation tissue and skin appendage generation in vivo, and the expression of related cytokines and proteins results proved that the multifunctional hydrogel had more promoting efficient in the mouse full-thickness skin defect repair model. We predict that the multifunctional CMC/HA-DA hydrogel shows great potential in the skin repairing and tissue regeneration.

#### Data availability statement

Data availability may be granted by contacting the corresponding author.

#### Credit author statement

LL. Cui: Investigation, Writing- Original draft preparation. JK. Li: Validation Investigation, Data curation. SM. Guan: Investigation, Software, Visualization. KX. Zhang: Writing- Reviewing and Editing. K. Zhang: Resources, Supervision, Methodology. JA. Li. Project administration, Conceptualization.

#### Declaration of competing interest

The authors declare that they have no known competing financial interests or personal relationships that could have appeared to influence the work reported in this paper.

#### Acknowledgement

This research was funded by the National Natural Science Foundation of China (U2004164).

#### Appendix A. Supplementary data

Supplementary data to this article can be found online at <https://doi.org/10.1016/j.mtbio.2022.100257>.

#### References

- J. Tam, Y. Wang, L.N. Vuong, J.M. Fisher, W.A. Farinelli, R.R. Anderson, Reconstitution of full-thickness skin by microcolumn grafting, *J. Tissue. Eng. Regen. Med.* 11 (10) (2017) 2796–2805.
- R. Papini, Management of burn injuries of various depths, *BMJ* 329 (7458) (2004) 158–160.
- R. Fu, C. Li, C. Yu, H. Xie, S. Shi, Z. Li, Q. Wang, L. Lu, A novel electrospun membrane based on moxifloxacin hydrochloride/poly(vinyl alcohol)/sodium alginate for antibacterial wound dressings in practical application, *Drug Deliv.* 23 (3) (2016) 828–839.
- W. Oualla-Bachiri, A. Fernández-González, M.I. Quiñones-Vico, S. Arias-Santiago, From grafts to human bioengineered vascularized skin substitutes, *Int. J. Mol. Sci.* 21 (21) (2020) 8197.
- A.R. Abbasi, M. Sohail, M.U. Minhas, T. Khaliq, M. Kousar, S. Khan, Z. Hussain, A. Munir, Bioinspired sodium alginate based thermosensitive hydrogel membranes for accelerated wound healing, *Int. J. Biol. Macromol.* 155 (2020) 751–765.
- B. Hou, M. Qi, J. Sun, M. Ai, X. Ma, W. Cai, Y. Zhou, L. Ni, J. Hu, F. Xu, L. Qiu, Preparation, characterization and wound healing effect of vaccarin-chitosan nanoparticles, *Int. J. Biol. Macromol.* 165 (2020) 3169–3179.
- H. Sorg, D.J. Tilkorn, S. Hager, J. Hauser, U. Mirastschijski, Skin wound healing: an update on the current knowledge and concepts, *Eur. Surg. Res.* 58 (1–2) (2017) 81–94.
- N.T. Dai, H.I. Chang, Y.W. Wang, K.Y. Fu, T.C. Huang, J.K. Li, P.S. Hsieh, L.G. Dai, C.K. Hsu, P.K. Maitz, Restoration of skin pigmentation after deep partial or full-thickness burn injury, *Adv. Drug Deliv. Rev.* 123 (2018) 155–164.
- K. Vig, A. Chaudhari, S. Tripathi, S. Dixit, R. Sahu, S. Pillai, V.A. Dennis, S.R. Singh, Advances in skin regeneration using tissue engineering, *Int. J. Mol. Sci.* 18 (4) (2017) 789.
- J.R. Yu, J. Navarro, J.C. Coburn, B. Mahadik, J. Molnar, J.H. Holmes, A.J. Nam, J.P. Fisher, Current and future perspectives on skin tissue engineering: key features of biomedical research, translational assessment, and clinical application, *Adv. Healthc. Mater.* 8 (5) (2019), e1801471.
- Y. Wu, J. Wang, L. Li, X. Fei, L. Xu, Y. Wang, J. Tian, Y. Li, A novel hydrogel with self-healing property and bactericidal activity, *J. Colloid Interface Sci.* 584 (2021) 484–494.
- E.A. Kamoun, R.S. Kenawy, X. Chen, A review on polymeric hydrogel membranes for wound dressing applications: PVA-based hydrogel dressings, *J. Adv. Res.* 8 (3) (2017) 217–233.
- Y. Tu, N. Chen, C. Li, H. Liu, R. Zhu, S. Chen, Q. Xiao, J. Liu, S. Ramakrishna, L. He, Advances in injectable self-healing biomedical hydrogels, *Acta Biomater.* 90 (2019) 1–20.
- M. Anamizu, Y. Tabata, Design of injectable hydrogels of gelatin and alginate with ferric ions for cell transplantation, *Acta Biomater.* 100 (2019) 184–190.
- J.E. Mealy, J.J. Chung, H.H. Jeong, D. Issadore, D. Lee, P. Atluri, J.A. Burdick, Injectable granular hydrogels with multifunctional properties for biomedical applications, *Adv. Mater.* 30 (20) (2018), e1705912.
- Y.P. Liang, J.H. He, B.L. Guo, Functional hydrogels as wound dressing to enhance wound healing, *ACS Nano* 15 (8) (2021) 12687–12722.
- D. Zhou, S. Li, M. Pei, H. Yang, S. Gu, Y. Tao, D. Ye, Y. Zhou, W. Xu, P. Xiao, Dopamine-modified hyaluronic acid hydrogel adhesives with fast-forming and high tissue adhesion, *ACS Appl. Mater. Interfaces* 12 (16) (2020) 18225–18234.
- M.F.P. Graça, S.P. Miguel, C.S.D. Cabral, I.J. Correia, Hyaluronic acid-Based wound dressings: a review, *Carbohydr. Polym.* 241 (2020) 116364.
- A.G. Tavianatou, I. Caon, M. Franchi, Z. Piperigkou, D. Galesso, N.K. Karamanos, Hyaluronan: molecular size-dependent signaling and biological functions in inflammation and cancer, *FEBS J.* 286 (15) (2019) 2883–2908.
- J. Webber, R.H. Jenkins, S. Meran, A. Phillips, R. Steadman, Modulation of TGFbeta1-dependent myofibroblast differentiation by hyaluronan, *Am. J. Pathol.* 175 (1) (2009) 148–160.
- R. Stern, A.A. Asari, K.N. Sugahara, Hyaluronan fragments: an information-rich system, *Eur. J. Cell Biol.* 85 (8) (2006) 699–715.
- H. Ying, J. Zhou, M. Wang, D. Su, Q. Ma, G. Lv, J. Chen, In situ formed collagen-hyaluronic acid hydrogel as biomimetic dressing for promoting spontaneous wound healing, *Mater. Sci. Eng. C. Mater. Biol. Appl.* 101 (2019) 487–498.
- Y. Liang, X. Zhao, T. Hu, B. Chen, Z. Yin, P.X. Ma, B. Guo, Adhesive hemostatic conducting injectable composite hydrogels with sustained drug release and photothermal antibacterial activity to promote full-thickness skin regeneration during wound healing, *Small* 15 (12) (2019), e1900046.
- A.I. Neto, A.C. Cibrão, C.R. Correia, R.R. Carvalho, G.M. Luz, G.G. Ferrer, G. Botelho, C. Picart, N.M. Alves, J.F. Mano, Nanostructured polymeric coatings based on chitosan and dopamine-modified hyaluronic acid for biomedical applications, *Small* 10 (12) (2014) 2459–2469.
- Y.Q. Liang, Z.L. Li, Y. Huang, R. Yu, B.L. Guo, Dual-dynamic-bond cross-linked antibacterial adhesive hydrogel sealants with on-demand removability for post-wound-closure and infected wound healing, *ACS Nano* 15 (4) (2021) 7078–7093.
- M. Li, Y.P. Liang, J.H. He, H.L. Zhang, B.L. Guo, Two-pronged strategy of biomechanically active and biochemically multifunctional hydrogel wound dressing, to accelerate wound closure and wound healing, *Chem. Mater.* 32 (23) (2020) 9937–9953.
- Y.P. Liang, X. Zhao, T.L. Hu, B.J. Chen, Z.H. Yin, P.X. Ma, B.L. Guo, Adhesive hemostatic conducting injectable composite hydrogels with sustained drug release and photothermal antibacterial activity to promote full-thickness skin regeneration during wound healing, *Small* 15 (12) (2019) 1900046.
- Q.H. Yu, C.M. Zhang, Z.W. Jiang, S.Y. Qin, A.Q. Zhang, Mussel-Inspired adhesive polydopamine-functionalized hyaluronic acid hydrogel with potential bacterial inhibition, *Glob. Chall.* 4 (2) (2020) 1900068.
- L. Koivusalo, M. Kauppila, S. Samanta, V.S. Parihhar, T. Ilmarinen, S. Miettinen, O.P. Oommen, H. Skottman, Tissue adhesive hyaluronic acid hydrogels for sutureless stem cell delivery and regeneration of corneal epithelium and stroma, *Biomaterials* 225 (2019) 119516.
- B.K. Ahn, Perspectives on mussel-inspired wet adhesion, *J. Am. Chem. Soc.* 139 (30) (2017) 10166–10171.
- Q.H. Yu, C.M. Zhang, Z.W. Jiang, S.Y. Qin, A.Q. Zhang, Mussel-Inspired adhesive polydopamine-functionalized hyaluronic acid hydrogel with potential bacterial inhibition, *Global Chall.* 4 (2020) 1900068.
- R. Wang, J.Z. Li, W. Chen, T.T. Xu, S.F. Yun, Z. Xu, Z.Q. Xu, T. Sato, B. Chi, H. Xu, A biomimetic mussel-inspired ε-Poly-L-lysine hydrogel with robust tissue-anchor and anti-infection capacity, *Adv. Funct. Mater.* (2017) 1604894.
- Y.J. Zhong, J. Wang, Z.Y. Yuan, Y. Wang, Z.H. Xi, L. Li, Z.Y. Liu, X.H. Guo, A mussel-inspired carboxymethyl cellulose hydrogel with enhanced adhesiveness through enzymatic crosslinking, *Colloids Surf. B Biointerfaces* 179 (2019) 462–469.
- D.D. Wang, P.P. Xu, S.S. Wang, W.L. Li, W.Z. Liu, Rapidly curable hyaluronic acid-catechol hydrogels inspired by scallops as tissue adhesives for hemostasis and wound healing, *Eur. Polym. J.* 134 (2020) 109763.
- D. Wang, N. Zhang, G. Meng, J. He, F. Wu, The effect of form of carboxymethyl-chitosan dressings on biological properties in wound healing, *Colloids Surf. B Biointerfaces* 194 (2020) 111191.

- [36] R. Jayakumar, M. Prabakaran, S.V. Nair, S. Tokura, H. Tamura, N. Selvamurugan, Novel carboxymethyl derivatives of chitin and chitosan materials and their biomedical applications, *Prog. Mater. Sci.* 55 (2010) 675–709.
- [37] H. Li, F. Cheng, X. Wei, X. Yi, S. Tang, Z. Wang, Y.S. Zhang, J. He, Y. Huang, Injectable, self-healing, antibacterial, and hemostatic N,O-carboxymethyl chitosan/oxidized chondroitin sulfate composite hydrogel for wound dressing, *Mater. Sci. Eng. C. Mater. Biol. Appl.* 118 (2021) 111324.
- [38] Y. Cheng, Z. Hu, Y. Zhao, Z. Zou, S. Lu, B. Zhang, S. Li, Sponges of carboxymethyl chitosan grafted with collagen peptides for wound healing, *Int. J. Mol. Sci.* 20 (16) (2019) 3890.
- [39] P. Campomanes, U. Rothlisberger, M. Alfonso-Prieto, C. Rovira, The molecular mechanism of the catalase-like activity in horseradish peroxidase, *J. Am. Chem. Soc.* 137 (34) (2015) 11170–11178.
- [40] T. Ma, L.X. Lv, C.Z. Ouyang, X.N. Hu, X.J. Liao, Y. Song, X.S. Hu, Rheological behavior and particle alignment of cellulose nanocrystal and its composite hydrogels during 3D printing, *Carbohydr. Polym.* 253 (2021) 117217.
- [41] C. Wang, M. Wang, T. Xu, X. Zhang, C. Lin, W. Gao, H. Xu, B. Lei, C. Mao, Engineering bioactive self-healing antibacterial exosomes hydrogel for promoting chronic diabetic wound healing and complete skin regeneration, *Theranostics* 9 (1) (2019) 65–76.
- [42] F. Oroojalian, Z. Jahanafrooz, F. Chogan, A.H. Rezayan, E. Malekzade, S.J.T. Rezaei, M.R. Nabid, A. Sahebkar, Synthesis and evaluation of injectable thermosensitive penta-block copolymer hydrogel (PNIPAAm-PCL-PEG-PCL-PNIPAAm) and star-shaped poly(CL–CO–LA)-b-PEG for wound healing applications, *J. Cell. Biochem.* 120 (2019) 17194–17207.
- [43] M. Yao, F. Gao, R. Xu, J. Zhang, Y. Chen, F. Guan, A dual-enzymatically cross-linked injectable gelatin hydrogel loaded with BMSC improves neurological function recovery of traumatic brain injury in rats, *Biomater. Sci.* 7 (10) (2019) 4088–4098.
- [44] Y. Zhong, J. Wang, Z. Yuan, Y. Wang, Z. Xi, L. Li, Z. Liu, X. Guo, A mussel-inspired carboxymethyl cellulose hydrogel with enhanced adhesiveness through enzymatic crosslinking, *Colloid. And. Surfaces. B. Biointerfaces.* 179 (2019) 462–469.
- [45] C. Fan, J. Fu, W. Zhu, D.A. Wang, A mussel-inspired double-crosslinked tissue adhesive intended for internal medical use, *Acta Biomater.* 33 (2016) 51–63.
- [46] X. Zhao, H. Wu, B. Guo, R.R. Dong, Y. Qiu, P.X. Ma, Antibacterial anti-oxidant electroactive injectable hydrogel as self-healing wound dressing with hemostasis and adhesiveness for cutaneous wound healing, *Biomaterials* 122 (2017) 34–47.
- [47] Q. Wei, J. Duan, G. Ma, W. Zhang, Q. Wang, Z. Hu, Enzymatic crosslinking to fabricate antioxidant peptide-based supramolecular hydrogel for improving cutaneous wound healing, *J. Mater. Chem. B.* 7 (2019) 2220–2225.
- [48] Z. Ahmadian, A. Correia, M. Hasany, P. Figueiredo, F. Dobakhti, M.R. Eskandari, S.H. Hosseini, R. Abiri, S. Khorshid, J. Hirvonen, H.A. Santos, M.A. Shahbazi, A hydrogen-bonded extracellular matrix-mimicking bactericidal hydrogel with radical scavenging and hemostatic function for pH-responsive wound healing acceleration, *Adv. Healthc. Mater.* 10 (3) (2021), e2001122.
- [49] S. Naahidi, M. Jafari, M. Logan, Y. Wang, Y. Yuan, H. Bae, B. Dixon, P. Chen, Biocompatibility of hydrogel-based scaffolds for tissue engineering applications, *Biotechnol. Adv.* 35 (5) (2017) 530–544.
- [50] X.C. Wang, P.X. Liu, Q.T. Wu, Z.Z. Zheng, M.B. Xie, G.Q. Chen, J. Yu, X.Q. Wang, G. Li, D. Kaplan, Sustainable antibacterial and anti-inflammatory silk suture with surface modification of combined-therapy drugs for surgical site infection, *ACS Appl. Mater. Interfaces* 14 (9) (2022) 11177–11191.
- [51] M.F. Shih, M.D. Shau, M.Y. Chang, S.K. Chiou, J.K. Chang, J.Y. Cherng, Platelet adsorption and hemolytic properties of liquid crystal/composite polymers, *Int. J. Ophthalmic. Pract.* 327 (1–2) (2006) 117–125.
- [52] C. Wang, H. Niu, X. Ma, H. Hong, Y. Yuan, C. Liu, Injectable, quaternized hydroxyethyl cellulose composite hydrogel coordinated by mesocellular silica foam for rapid, noncompressible hemostasis and wound healing, *ACS Appl. Mater. Interfaces* 11 (38) (2019) 34595–34608.
- [53] N. Rajabi, M. Kharaziha, R. Emadi, A. Zarrabi, H. Mokhtari, S. Salehi, An adhesive and injectable nanocomposite hydrogel of thiolated gelatin/gelatin methacrylate/Laponite® as a potential surgical sealant, *J. Colloid Interface Sci.* 564 (2020) 155–169.
- [54] C. Wang, Y. Chen, Y. Wang, X. Liu, Y. Liu, Y. Li, H. Chen, C. Fan, D. Wu, J. Yang, Inhibition of COX-2, mPGES-1 and CYP4A by isoliquiritigenin blocks the angiogenic Akt signaling in glioma through ceRNA effect of miR-194-5p and lncRNA NEAT1, *J. Exp. Clin. Cancer Res.* 38 (1) (2019) 371.
- [55] W. Wang, C. Yang, X.Y. Wang, L.Y. Zhou, G.J. Lao, D. Liu, C. Wang, M.D. Hu, T.T. Zeng, L. Yan, M. Ren, MicroRNA-129 and -335 promote diabetic wound healing by inhibiting sp1-mediated MMP-9 expression, *Diabetes* 67 (8) (2018) 1627–1638.
- [56] Y.C. Chuang, M.C. Cheng, C.C. Lee, T.Y. Chiou, T.Y. Tsai, Effect of ethanol extract from *Lactobacillus plantarum* TWK10-fermented soymilk on wound healing in streptozotocin-induced diabetic rat, *Amb. Express* 9 (1) (2019) 163.
- [57] Y. Tang, M. Hu, Y. Xu, F. Chen, S. Chen, M. Chen, Y. Qi, M. Shen, C. Wang, Y. Lu, Z. Zhang, H. Zeng, Y. Quan, F. Wang, Y. Su, D. Zeng, S. Wang, J. Wang, Megakaryocytes promote bone formation through coupling osteogenesis with angiogenesis by secreting TGF- $\beta$ 1, *Theranostics* 10 (5) (2020) 2229–2242.
- [58] Y.P. Liang, X. Zhao, T.L. Hu, Y. Han, B.L. Guo, Mussel-inspired, antibacterial, conductive, antioxidant, injectable composite hydrogel wound dressing to promote the regeneration of infected skin, *J. Colloid Interface Sci.* 556 (2019) 514–528.
- [59] S.M. Guan, K. Zhang, L.L. Cui, J.H. Liang, J.A. Li, F.X. Guan, Injectable gelatin/oxidized dextran hydrogel loaded with apocynin for skin tissue regeneration, *Mater. Sci. Eng. C* (2021), <https://doi.org/10.1016/j.msec.2021.112604>.